Influence of the Pd−Si Ratio on the Valence Transition in $EuPd_2Si_2$ Single Crystals

Kristin Kliemt,* Marius Peters, Isabel Reiser, Michelle Ocker, Franziska Walther, Doan-My Tran, Eunhyung Cho, Michael Merz, Amir Abbas Haghighirad, Dominik C. Hezel, Franz Ritter, and Cornelius Krellner

ABSTRACT: Single crystals of intermediate valent $EuPd_2Si_2$ were grown from an Eu-rich melt by the Bridgman as well as the Czochralski technique. T he chemical and structural characterization of an extracted single crystalline Czochralski-grown specimen yielded a slight variation of the Si−Pd ratio along the growth direction and confirms t he e xistence o f a finite $Eu(Pd_{1-m}Si_m)_2Si_2$ homogeneity range. The thorough physical characterization carried out on the same crystal showed that this tiny variation in the composition affects t he t emperature T_v at which the valence transition occurs. T hese experiments demonstrate a strong coupling between structural and physical properties in the prototypical valence-fluctuating system $EuPd_2Si_2$ and explain the different reported values of T_v.

INTRODUCTION

The study of emergent phenomena due to strong electron−electron interactions is at the heart of research in condensed matter. For these types of systems, the coupling of electronic degrees of freedom to the lattice are usually not much in the focus of research. In recent years, however, more and more physical phenomena have arisen in materials which additionally show a strong coupling of the electronic degrees of freedom to the lattice. Examples are tetragonal iron-based superconductors, where a so-called collapsed tetragonal phase appears upon cooling or application of pressure which is connected to an abrupt change in the *c*-lattice parameter.[1] In the organic conductor κ-$(BEDT\text{-}TTF)_2Cu[N(CN)_2]Cl$, the breakdown of Hooke's law was observed in a certain pressure−temperature range at the Mott-metal insulator transition, and the appearance of critical elasticity was proposed.[2] In the past, intermetallic Eu systems were studied due to the intermediate valent nature of Eu in these compounds. The change of the Eu valence can be tuned by temperature[3] and/or pressure.[4] Nowadays, these compounds attract attention due to the large volume changes accompanied by the valence transition. Eu can occur in different valence states which are very close in energy. The magnetic $Eu^{(2+\delta)+}$ ($4f^7$ configuration) leading to a larger unit cell volume, appears at low pressures and high temperatures, whereas the nonmagnetic $Eu^{(3-\delta')+}$ ($4f^6$ configuration) leading to a smaller unit cell volume is adopted at high pressures and low temperatures. In a general phase diagram, the two regions are separated at low temperatures by a line of first-order valence transitions.[5] Of special interest are intermediate-valent Eu-122 compounds which can be tuned by pressure (temperature) toward the second order critical end point of the line of the first order valence transitions. In particular, $EuPd_2Si_2$ is proposed to be located very close to the critical pressure in the generic phase diagram. The extrapolation of results obtained on polycrystalline samples yielded that $EuPd_2Si_2$ is located on the high-pressure side of the critical end point.[6,7] It is expected that in $EuPd_2Si_2$ critical elasticity meaning a strong lattice softening and nonlinear strain−stress relations might occur as well.

First reports on $EuPd_2Si_2$ appeared in the 1980s where the intermediate-valent nature of Eu was studied. Here, a strong temperature dependence of the ^{151}Eu Mössbauer isomer shift together with a maximum in the temperature dependence of the magnetic susceptibility was observed for the first time in a Eu-based intermediate valent compound.[8] The rare earth ion undergoes a valence transition from $Eu^{2.2+}$ at room temperature to $Eu^{2.9+}$ in the bulk at low temperature $\leq$100 K, while photoemission spectroscopy revealed divalent Eu at the surface in the whole temperature range.[3,8,9] The increase of the Eu valence in the bulk upon cooling strongly influences the lattice parameters. In particular, it causes a change of the *a* parameter

while the c parameter remains nearly unchanged. The analysis of the Bragg line-widths shows a broadening of the (200) and therefore suggested the existence of a temperature dependent distribution of a parameters in powder samples.[10] A valence transition can be induced not only by decreasing the temperature but also by applying pressure which was revealed first by electrical resistivity and thermoelectric power measurements.[11] Later on, from the temperature as well as the pressure dependence of the electrical resistivity, the linear compressibility, and the thermal expansion, a pressure−temperature (p-T) phase diagram was constructed by Batlogg et al.[6] From these data it was concluded that $EuPd_2Si_2$ shows a continuous phase transition and is situated near the critical end point of a line of first order phase transitions in the p-T diagram. It was proposed that this end point could be reached by applying low negative chemical pressure, for instance, via substitution of the smaller Pd atoms by larger Au atoms.[12] It was shown by Mössbauer effect measurements that the transition becomes first order when applying negative chemical pressure as, for instance, for $x > 0.1$ in $Eu(Pd_{1-x}Au_x)_2Si_2$.[13] $EuPd_2Si_2$ was studied by neutron scattering and by measurements of the magnetic susceptibility. It turned out that the tail in the static susceptibility at low temperatures can be caused by the ordering of a magnetic secondary phase.[14] Although $EuPd_2Si_2$ is one of the prototypical valence-fluctuating systems, previous studies were mostly carried out on polycrystalline samples. It should be mentioned that the crystal growth of Eu compounds is challenging due to the high vapor pressure of Eu and its affinity to oxygen. Only recently have small single crystals of $EuPd_2Si_2$ grown by the Bridgman method become available.[5] The comparison of poly- and single-crystal heat capacity data from different sources[5,15] shows sample dependencies concerning the temperature at which the valence transition occurs. From this fact, one might speculate that $EuPd_2Si_2$ is a compound that exists in a homogeneity range as already found for the related material $ErPd_2Si_2$.[16] In ref 17 an $EuPd_{2-x}Si_{2+x}$ alloy series was studied; the respective samples were prepared by arc-melting followed by an annealing step. The samples studied contained either secondary phases or grain boundaries where magnetic impurities accumulated. Due to this fact, the information that can be gained from their magnetic characterization is limited. This motivates further attempts to grow single crystals with a minimum of magnetic inclusions which enable studies of the physical properties in connection with the study of the structural details of the material in a reliable manner.

We used the Czochralski method to provide large and pure single crystals of $EuPd_2Si_2$ and studied the influence of the Pd−Si composition change in a sample on its physical properties. In future studies, this will help figuring out whether the scenario of critical elasticity,[18] which was recently proposed for the Mott transition in κ-$(BEDT\text{-}TTF)_2Cu[N(CN)_2]Cl$, can be found in $EuPd_2Si_2$.

EXPERIMENTAL DETAILS

A Simultaneous Thermal Analysis device (STA 449 C, Netzsch), which allows simultaneous thermogravimetry (TG) and differential thermal analysis (DTA), was used to get insight in the solidification process of an Eu-enriched starting stoichiometry. DTA under Ar flow of 150 mL/min was done with a heating/cooling rate of 10 K/min using the different stoichiometries Eu:Pd:Si = 1.4:2:2 ($Eu_{1.4}$, Figure 1) and Eu:Pd:Si = 1.5:2:2 ($Eu_{1.5}$) in Al_2O_3 and graphite crucibles. We observed a strong evaporation of Eu leading to a weight loss of up to 2.5% and a reaction with the Pt wires of the thermocouple.

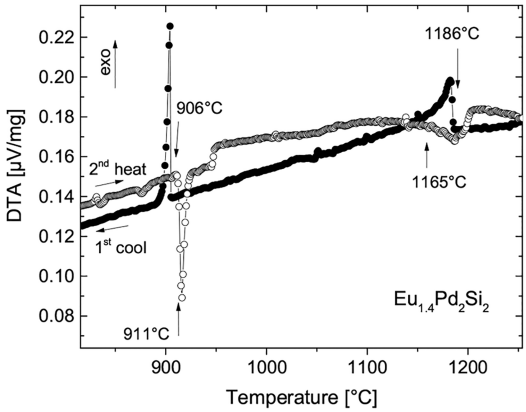

Figure 1. DTA experiment performed for the initial stoichiometry of Eu:Pd:Si = 1.4:2:2 ($Eu_{1.4}$). Two signals were observed upon cooling (closed circles)/heating (open circles) corresponding to the solidification/melting of $EuPd_2Si_2$ at around 1180 °C and the remaining flux at lower temperatures.

Furthermore, we found that the Al_2O_3 crucible was attacked by the melt and that Al was incorporated in the sample. The DTA signal of the second cooling from a run in a graphite crucible (sample EC05) (Figure 1) shows two features: one which indicates the solidification of $EuPd_2Si_2$ in the flux at 1186 °C for the $Eu_{1.4}$ sample (1205 °C for $Eu_{1.5}$) and a second which belongs to the solidification of the flux itself at 906 °C. For the crystal growth from a Eu-rich melt, high purity elements Eu (99.99%, chunks, Alfa Aesar), Pd (99.999%, rod, Heraeus), and Si (99.99%, pieces, Cerae) were used in a ratio of Eu:Pd:Si = 1.5:2:2 as proposed in ref 5. The Bridgman growth was done from the elements in a vertical resistive furnace (GERO HTRV70−250/18). Since the crucible material tantalum was attacked by the melt, we used an additional graphite inner crucible.

The Czochralski growth was done using prereacted material with a total weight of up to 15 g. The initial stoichiometry varied from $Eu_{1.2-1.5}Pd_2Si_2$. In the first step, the binary compound PdSi (≈900 °C) was prepared by arc melting, to reduce the high melting points T_m of Pd (1555 °C) and Si (1414 °C). Afterward, using a glovebox, this material together with elementary Eu (T_m = 822 °C) was put in a glassy carbon inner crucible and enclosed in a niobium outer crucible. We used a box furnace (Linn) to heat the precursor up to 835 °C under Ar flow. The Czochralski crystal growth was done in an Arthur D. Little growth chamber equipped with a high-frequency generator from Hüttinger. The chamber was filled with an Ar pressure of 20 bar to slow down the evaporation of Eu at high temperatures. The air-sensitive precursor was quickly put in a cold copper crucible of a levitation setup followed by an extended purging to remove oxygen. This setup enables a quasi crucible-free crystal growth from a levitating melt which is necessary due to the strong reaction of the melt with any tested crucible material. For this study, samples from three different Czochralski growth experiments #1 (MP401), #2 (MP413a), and #3 (MP413b) were investigated. We used powder X-ray diffraction (PXRD, Cu K_α radiation) to check the lattice parameters of crushed single crystals and their T dependence, and energy—as well as wavelength-dispersive X-ray spectroscopy (EDX, WDX) to determine the chemical composition of the crystals.

EDX measurements were performed at the Kristall- and Materiallabor, Goethe Universität Frankfurt, using a scanning electron microscope, Zeiss DSM 940 A, with an additional energy dispersive detector (EDAX Ametek GmbH). At the KIT, the chemical composition of the crystals was examined by energy-dispersive X-ray spectroscopy employing a Coxem EM-30^N benchtop scanning electron microscope equipped with an Oxford Instruments detection system. WDX measurements were performed with a JEOL-8530F Plus Hyperprobe at the Institut für Geowissenschaften, Goethe Universität Frankfurt. Individual points were measured with 3 μm spot sizes at an acceleration voltage of 20 kV and a current of 30 nA,

with counting times of 30 s (peak) and 15 s (background). Pure Si and Pd metals as well as a Eu-Phosphate ($EuPO_4$) were used as standards. As some oxidation of the standards cannot be excluded, some minor systematic shift of the measured concentrations (typically below 0.2 rel.% for Pd and Si, and up to 1.5 rel.% for Eu) can not be excluded. Internal reproducibility is typically below 0.5 rel.%. For a more detailed structural characterization, X-ray diffraction (XRD) data on representative $Eu(Pd_{1-m}Si_m)_2$ single-crystal samples were collected at 295 K on a STOE imaging plate diffraction system (IPDS-2T) using Mo K_α radiation. All accessible reflections (≈5000) were measured up to a maximum angle of $2\Theta = 65°$. The data were corrected for Lorentz, polarization, extinction, and absorption effects. Using SHELXL[19] and JANA2006,[20] all averaged symmetry-independent reflections ($I > 2\sigma$) have been included for the respective refinements in the tetragonal space group (SG) *I*4/*mmm*. For all compositions, the unit cell and the space group were determined, the atoms were localized in the unit cell utilizing random phases as well as Patterson superposition methods, the structure was completed and solved using difference Fourier analysis, and finally the structure was refined. In all cases the refinements converged quite well and show excellent reliability factors (see GOF, R_1, and wR_2 in Table 1).

The samples *E*0, *E*4, and *E*8 for the single crystal XRD analysis were extracted from the Czochralski grown sample #3 at distances of 2.5 mm, 7 mm, and 11 mm below the seed. Low-temperature PXRD was done in a Siemens D500 diffractometer (Cu K_α radiation). A Laue camera with X-ray radiation from a tungsten anode was used to determine the orientation of our single crystals and to localize grain boundaries in the Czochralski grown samples. Heat capacity, four-point resistivity, and magnetization measurements were performed using the commercial measurement options of a Quantum Design PPMS.

RESULTS

Crystal Growth. The DTA experiments (Figure 1) showed that the compound solidifies in flux already at about 1200 °C at the initial weight stoichiometry of Eu:Pd:Si = 1.4:2:2. This means that the growth temperatures can be chosen significantly lower than previously assumed and used for Bridgman growth[5] if a pre-reacting step is carried out. Both types of samples prepared by DTA and by Bridgman method showed a large amount of included secondary phases. Furthermore, these samples displayed a very broad transition in the specific heat above 100 K. The valence transition temperatures which were determined by heat capacity and magnetization measurements exhibited strong sample dependencies. During reproduction experiments using the Bridgman method, it was noticed that the grown crystals were, on one hand, small (platelets, ≈1 mm × 1.5 mm) and on the other hand also contained many Eu-rich flux inclusions, which motivated us to develop the growth of this compound using the Czochralski method. The Czochralski growth of $EuPd_2Si_2$ is highly challenging: (i) Eu has a high vapor pressure at high temperatures, (ii) the melt attacks all tested crucible materials (tantalum, Al_2O_3, graphite, glassy carbon) at high temperatures, and (iii) the ideal starting stoichiometry for obtaining inclusion-free samples is unknown so far. We performed 10 crystal growth experiments, each of which consisted of the pre-reaction steps followed by Czochralski growth. In all experiments, rod-shaped seeds were used with the long edges cut in a crystallographic direction perpendicular to the *c*-direction. Using these seeds, all samples were pulled out of the melt in a direction perpendicular to the *c* direction. A typical growth result at the end of the optimization process is shown in Figure 2a). During the optimization of the growth process, it was found that the evaporation of Eu from the melt can be slowed sufficiently by an Ar overpressure of 20 bar in the growth chamber. Due to the high reactivity of the melt, the growth was carried out from the levitating melt. We observed that the higher the Eu content, the larger the proportion of the target phase that can be drawn from the melt. The optimization process revealed that up to an initial stoichiometry of Eu:Pd:Si = 1.45:2:2, the $EuPd_2Si_2$ phase is the first to crystallize. Higher Eu contents lead to unstable conditions during the seeding phase which is possibly caused by the formation of a different phase at the beginning of the growth process.

Table 1. Crystallographic Data of $Eu(Pd_{1-m}Si_m)_2Si_2$ at 295 K for Representative Samples *E*0, *E*4, and *E*8 Determined from Single-Crystal X-ray Diffraction[a]

	*E*0	*E*4	*E*8
space group	*I*4/*mmm*	*I*4/*mmm*	*I*4/*mmm*
a (Å)	4.2392(6)	4.2406(5)	4.2408(7)
c (Å)	9.8674(12)	9.8690(11)	9.8631(12)
α (deg)	90	90	90
β (deg)	90	90	90
γ (deg)	90	90	90
V (Å^3)	177.3	177.5	177.4
	Eu		
Wyck.	2*a*	2*a*	2*a*
x	0	0	0
y	0	0	0
z	0	0	0
U_{iso} (Å^2)	0.00898(14)	0.00786(11)	0.00836(12)
	Pd/Si		
Wyck.	4*d*	4*d*	4*d*
x	1/2	1/2	1/2
y	0	0	0
z	1/4	1/4	1/4
occ. (%)	97.0/3.0(5)	98.1/1.9(4)	98.8/1.2(5)
U_{iso} (Å^2)	0.00978(13)	0.00889(10)	0.00943(13)
	Si		
Wyck.	4*e*	4*e*	4*e*
x	0	0	0
y	0	0	0
z	0.37783(19)	0.37754(14)	0.37719(23)
U_{iso} (Å^2)	0.01039(35)	0.00897(27)	0.00947(34)
GOF	1.90	1.47	1.38
wR_2 (%)	4.15	3.20	3.33
R_1 (%)	1.72	1.24	1.21
	bond lengths		
Eu−Si (Å)	3.2309(9)	3.2330(7)	3.2341(11)
(Pd,Si)-Si (Å)	2.4665(11)	2.4657(8)	2.4637(13)
Si−Si (Å)	2.4110(30)	2.4170(19)	2.4220(28)

[a]For all compositions the structure was refined in the tetragonal space group (SG) *I*4/*mmm*. U_{iso} denotes the isotropic atomic displacement parameters (ADP). The ADPs were refined anisotropically but due to space limitations only the U_{iso} are listed in the table. The Wyckoff positions (Wyck.) are given as well. While for all samples the 4*e* Wyckoff position is completely occupied with Si, a certain amount of up to 3% Si is found on the Pd site (Wyckoff position 4*d*). Furthermore, some selected bond distances are depicted as well. Errors shown are statistical errors from the refinement.

Structural and Chemical Characterization. PXRD confirmed the $ThCr_2Si_2$ structure of the samples with lattice parameters at 300 K of a = 4.2396(5) Å and c = 9.8626(4) Å which is in good agreement with the literature.[4] Low-temperature PXRD was performed on a Czochralski grown

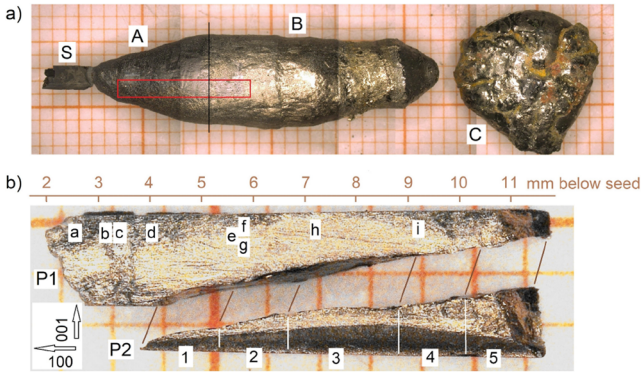

Figure 2. (a) Sample #3 grown by the Czochralski method using a single crystalline seed S. The upper part A of the sample is free from macroscopic inclusions, while the lower part B contains flux inclusions which are visible in the SEM picture. The residual flux C is not stable in air and decomposes after a few hours in air. (b) Single crystalline piece which was extracted from the sample (red box) shown in (a). The extracted crystal was divided into two different samples P1 and P2. Sample P1 was used for resistivity measurements at positions a−i and was characterized by single crystal XRD analysis, EDX and WDX. Sample P2 was cut into pieces 1−5 whose magnetization and heat capacity was measured.

sample #2 between 100 and 300 K (Figure 3a). For this sample, a large shift of the (103), the (112), and the (200) reflections was observed between 120 and 170 K. The (004) reflection exhibits only a small change of its position. Figure 3b,c shows the temperature dependent volume and the lattice parameters of samples from two different Czochralski growth experiments #1 (closed symbols) and #2 (open symbols). The lattice parameter a changes about 2%, while the length of the c parameter remains nearly unchanged in the studied temperature range. The full width at half-maximum (FWHM) of two reflections was analyzed by fitting their shapes with Gauss and Lorentz line shape. Our analysis of the (516) and the (004) reflections, shown in Figure 3d, yields no change of the FWHM upon cooling. From this we can conclude that no peak broadening of these reflections appears. Low-temperature PXRD was additionally performed on a sample grown by the Bridgman method (see Supporting Information S1). In this case, we found a broadening of the (112) peak between 140 and 130 K. Such a peak broadening was already observed in ref 10 and assigned to a distribution of a lattice parameters in the sample. Since the physical properties reported in the literature so far show a sample dependence, we performed the single crystal XRD analysis, the WDX and the EDX analysis very carefully to find deviations from the ideal 122 stoichiometry. Prior to EDX analysis, we examined the sample by scanning electron microscopy (SEM) for visible flux inclusions. We found that the sample was free of inclusions up to a length of ≈8.5 mm below the seed. The EDX analysis was performed on a longitudinal section for which a long rod-shaped single crystal (P1) (Figure 2b) was cut out of the grown sample #3. This sample was finely polished for the analysis. The analysis of this longitudinal section showed that the Eu content remained constant over the entire length of the sample studied. Furthermore, we found a small shift in the stoichiometry for Pd and Si within the first 8.5 mm of the sample. While the Pd content slightly increases, the Si content decreases at the same time. At a distance larger than 8.5 mm from the seed, no reliable statements can be made about the stoichiometry of the sample, since in this area the content of flux inclusions increases as can be seen in Figure 4c. The analysis of the side phase stoichiometry can be found in the Supporting Information S2. The first hint for a slight change of the Pd−Si ratio in the grown samples came from the EDX analysis. Subsequently, to get a quantitative statement, we performed a WDX analysis on the same sample and could verify this observation for the longitudinal analysis (Figure 4a). At a distance of 3 mm below the seed, we determined a ratio of Eu:Pd:Si = 20.5:40.5:39, while a ratio of Eu:Pd:Si = 20.5:41:38.5 at a distance of 11 mm was found. We additionally investigated radial lines of the sample (Figure 4b) and found the same trend. Concerning the reproducibility, the error is smaller than the size of the symbols used in Figure 4a,b. To get a better insight in how this slight change of the composition might influence the bond lengths, we performed a single crystal XRD analysis on small single crystals extracted from the same sample #3. The single crystal XRD analysis yields that while for all samples the 4*e* Wyckoff position is completely occupied with Si, a certain amount of up to 3% Si is found on the Pd site (Wyckoff position 4*d*). With decreasing Si content on the Pd site, the (Pd,Si)-Si bond length slightly decreases, while the Eu−Si and the Si−Si distances along the crystallographic c direction are slightly increasing. Moreover, the z parameter of the Si site (Wyckoff position 4*e*) is directly correlated to the changes in the amount of Si on the Pd site (see Table 1). We like to mention that the observed differences in the structure are at the limit of what can be resolved with XRD and can be reliably given only in the context of measurements on a whole series of samples, as was done here.

In our DTA, Bridgman and Czochralski growth experiments, we found different compositions of the included or remaining flux according to an EDX analysis. In DTA experiments, a silver-looking phase Eu:Pd:Si = 26.4:28.1:45.5 was found besides the main phase. In Bridgman growth experiments, the flux consisted of Eu, Eu:Pd:Si = 1:1:1 and Eu:Pd:Si = 31.2:41.2:27.5. In the Czochralski experiments we always found that the remaining material decomposed in air, and the determination of its composition was impossible.

Magnetic Susceptibility. The magnetic susceptibility (Figure 5), measured with B = 0.1T, $B \perp c$, shows a strong change of the slope in the valence transition region. The valence transition temperature T_v of a sample can be determined directly from the inflection point of the susceptibility curve. It is known from previous work that minor phases and impurities leave strong traces in the magnetization. Magnetization measurements are thus a sensitive tool to detect the presence of magnetic impurity phases. The magnetization of $EuPd_2Si_2$ was measured on 5 pieces, (1)−(5), whose exact extraction position from the sample is known (P2, Figure 2b). From these measurements, we can conclude two different trends. (i) The smaller the distance from the seed of a piece in the sample, the lower T_v. (ii) The amount of impurity contaminations, seen at low temperatures, increases with larger distance from the seed. If the content of side phases is very high, then the side phase signal influences the susceptibility so strongly that the inflection point in the susceptibility at T_v shifts or can no longer be determined. The gray curve (0) in Figure 5 exemplarily shows the susceptibility of a sample extracted at a distance of about 0.5 mm below the seed. The data show that the valence transition temperature is lowest for this sample. Furthermore, we observed for these early grown parts of the

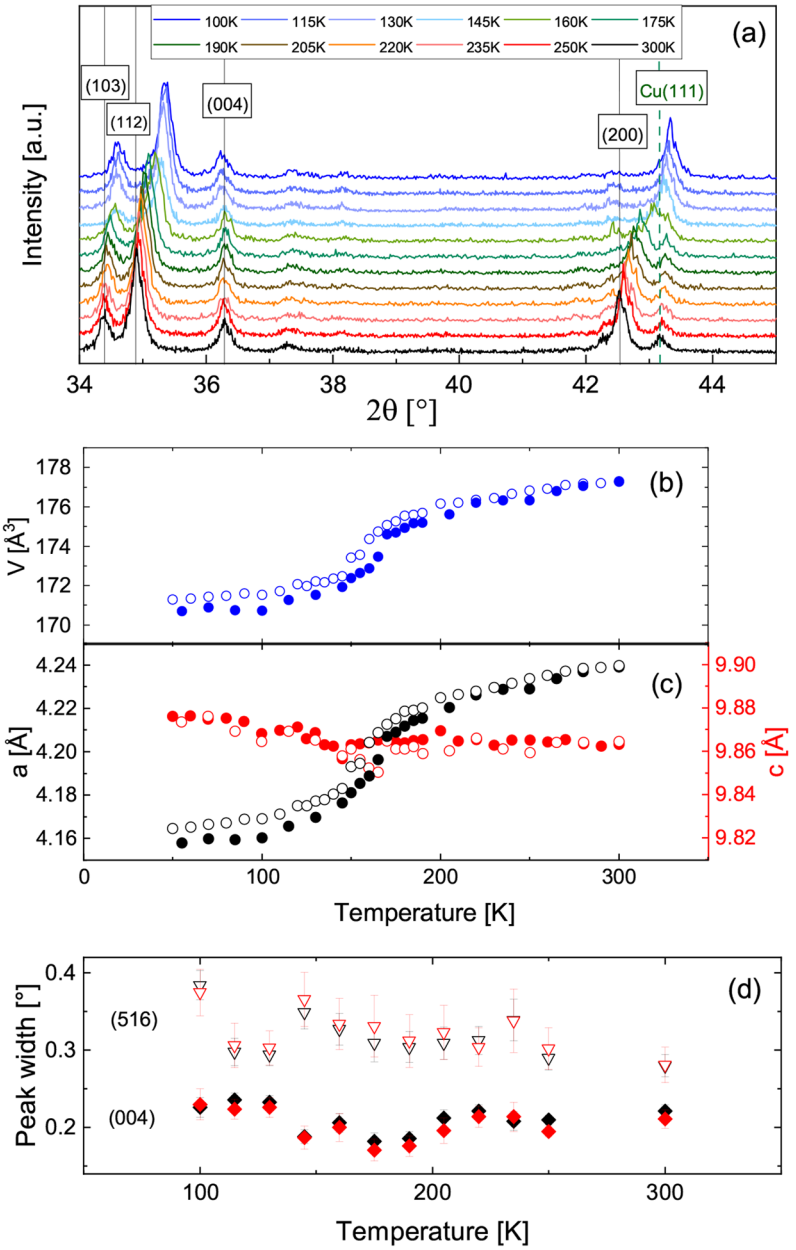

Figure 3. (a) Low-temperature powder X-ray diffraction between 100 and 300 K performed on a Czochralski grown sample #2. The green dashed line marks the position of the (111) reflex of Cu from the sample holder which serves as standard. Change of the volume of the unit cell (b) and the lattice parameters (c) with temperature for Czochralski grown samples #1 (closed symbols) and #2 (open symbols). (d) FWHM of the (516) and the (004) reflex fitting a Gaussian (black symbols) or Lorentzian line shape (red symbols) for sample #1.

sample a change of the characteristics of the impurity contribution at low temperatures compared to pieces (1)−(5). Samples (1) and (2) show a small increase of the susceptibility below 20 K which might be assigned to a paramagnetic defect contribution.[21] Samples (3)−(5) contain a side phase with a magnetic transition at about 10 K which might correspond to the ordering of Eu_2PdSi_3.[22] Contributions to the susceptibility below 100 K were already assigned to inclusions of magnetic side phases in this material in the past.[14]

Heat Capacity. The heat capacity of $EuPd_2Si_2$ shows a peak at the valence transition. It is known from the literature that T_v determined from heat capacity data is sample dependent: A polycrystalline sample showed T_v = 142 K,[15] while on a single crystalline sample T_v = 167 K was determined.[5] To systematically investigate this sample dependence and also to look for latent heat as an indication of a first order phase transition, we performed heat capacity measurements on the same samples (1)−(5) of piece P2 (Figure 2b), where the magnetization was measured. It was found that the position of the inflection point in the magnetization coincides with the position of the peak in the specific heat (Figure 6). Thus, in the heat capacity one also observes a dependence of the valence transition temperature on the position of extraction from the grown sample ranging from T_v = 142−154 K. It has to be mentioned that in other Czochralski grown samples an even lower T_v was detected. None of the samples investigated so far showed signs of a first order phase transition.

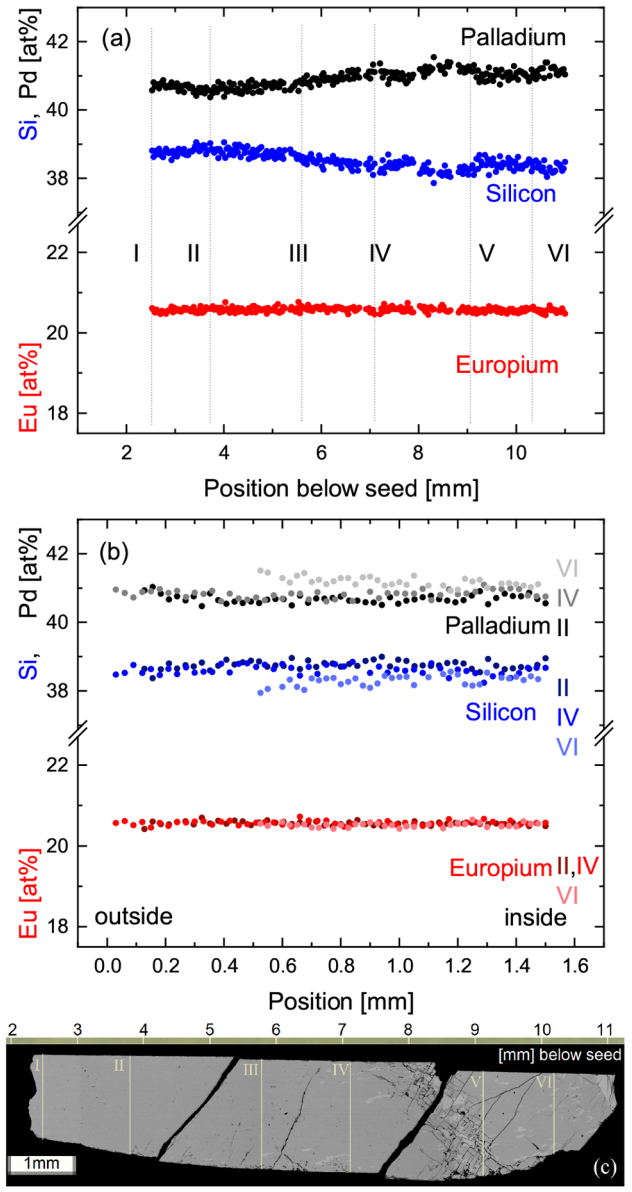

Figure 4. WDX was measured on the polished surface of (a) a longitudinal cut through the sample P1, shown in Figure 2b and part c in this graphic. In the upper part of the sample (A), we observed a constant Eu content but a slight change of the Pd−Si ratio in the first ≈8.5 mm. In the lower part (B) the sample contains macroscopic flux inclusions and the measured stoichiometry is not reliable. In (b) the analysis along the radial lines II, IV, and VI is shown (positions marked in part c)). (c) Electron microscope image of the polished sample which was analyzed with WDX.

Electrical Resistivity. The temperature dependence of the electrical resistivity, $\rho(T)$ (Figure 7), was systematically measured on a long rod-shaped sample at different positions (a−i, Figure 2b)) along the sample P1. The different positions of the contacts correspond to different distances from the seed. We observed that the measurements with current flow perpendicular to the *c*-direction succeeded only in a few cases. This was possibly related to a damage to the sample due to the strong change of the *a* lattice parameter. In many cases it was not possible to obtain reliable data. For position i which is already in the region with macroscopic flux inclusion we observe a different shape of the curve and a large hysteresis due

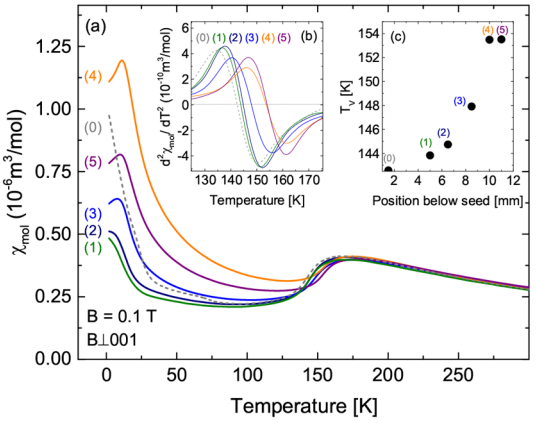

Figure 5. (a) The temperature dependence of the magnetic susceptibility was measured on different samples P2, (1)−(5) and (0). (b) The valence transition temperature T_v was determined from the second derivative of the susceptibility. (c) T_v depends on the extraction position of a sample from the grown crystal; see Figure 2b.

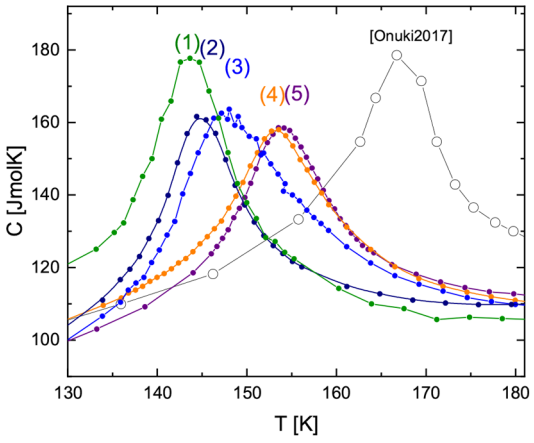

Figure 6. Temperature dependence of the heat capacity measured on samples P2, (1)−(5) (see Figure 2b) in comparison with data on single crystals from ref 5.

to the possible damaging of the sample during the temperature change. However, the measurement of the resistivity with $j \parallel c$ was possible in most cases. We observed a shift in the maximum for different contact positions a−h on sample P1 (Figure 7a). The temperature at which the maximum occurs (Figure 7b) depends on the contact position. The resistivity ratio $RR_{1.8K} = \rho(300\ K)/\rho(1.8\ K)$ varies between $RR_{1.8K} = 3.7$ (position (a)) and $RR_{1.8K} = 5.9$ (position (h)). For $j \parallel c$, we observed a small increase in the resistivity at T_v followed by a sharp drop toward low T during cooling. The curve shape between the two current directions differs only slightly. For $j \perp c$, black curve, *x*, in Figure 7c, the resistivity curve shows a similar characteristics at T_v but a lower residual resistivity ratio of $RR_{1.8\ K} \approx 2.5$.

DISCUSSION

The growth of Eu-based systems as single crystals is challenging mainly due to the incongruent solidification of the materials and the strong tendency of Eu to oxidize. In this work, we developed a process for growing crystals of $EuPd_2Si_2$ by the Czochralski method. We found that with an initial stoichiometry of Eu:Pd:Si = 1.45:2:2, the $EuPd_2Si_2$ phase is the

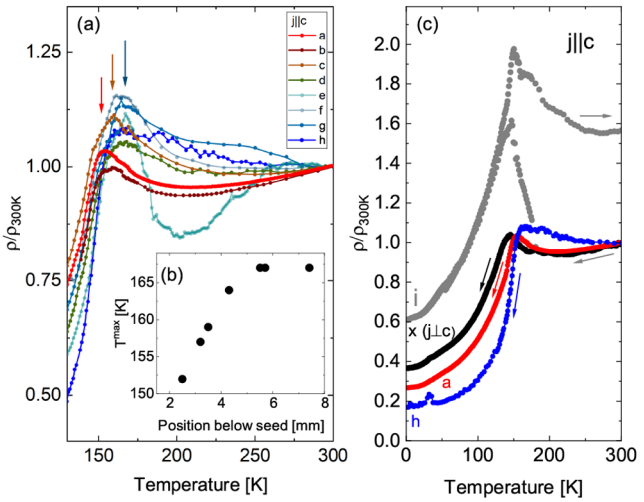

Figure 7. (a) The temperature dependence of the electrical resistivity was measured on different positions a–i (see Figure 2b) on one large single crystal P1 with current parallel to the *c*-direction. The arrows mark the position of the maximum which shifts for different contact positions. (b) The temperature T_{max} was determined from the maximum in the resistivity. (c) Electrical resistivity measured at contact positions a, h, i which shows a change of the shape of the curve. Curve x (black) shows the data obtained for $j \perp c$.

first to crystallize from the melt. We performed the structural and chemical characterization to compare the properties of our samples with those reported in the literature for powder samples and Bridgman grown single crystals. Low temperature PXRD experiments, performed between 300 and 10 K on Czochralski grown samples, showed that the *a* parameter undergoes a large change of about 2% upon cooling, while the *c* parameter remains almost constant. The valence transition manifests itself in a strong shift of the reflections, which can be observed, e.g., at the (200) reflection. In contrast, for a Bridgman grown sample we found a peak broadening for the (200) reflection similar to what was reported in ref 10. For the purer Czochralski grown samples, no peak broadening is observable which shows that this is not an intrinsic property of this material. The chemical characterization by WDX yielded that during the Czochralski growth process the compound solidifies in a homogeneity range $Eu(Pd_{1-m}Si_m)_2Si_2$. The analysis confirmed small changes in the Pd:Si ratio in the order of 1 at. % along the growth direction of the crystal. Although the systematic error in the absolute values might be larger than that change the relative trend is robust among different measurements. To get more microscopic insight into the structural variations, in parallel we conducted a single crystal XRD analysis on samples which were extracted from the same grown ingot. The careful analysis of different single crystals showed that the Pd site is partially occupied by Si which is accompanied by a small change of the Si position and correspondingly in the bond distances. The small change in the Pd–Si ratio accompanied by the change in the bond lengths has a large impact on the temperature T_v at which the valence transition occurs. In the electrical resistivity, measured with current parallel to the *c* direction on the same crystal used for the WDX analysis, we found maxima in the range 152 K $\leq T_{max} \leq$ 167 K. The neighboring part of that crystal was used to determine the valence transition from thermodynamic quantities. We determined 142 K $\leq T_v \leq$ 154 K from the inflection point in the magnetic susceptibility and heat capacity measurements showed that the peak temperature corresponds to T_v determined from the magnetic susceptibility. From this thorough analysis of the structural and physical properties, we conclude that with increasing distance to the seeding crystal, the stoichiometry of $EuPd_2Si_2$ moves toward the ideal 122 composition, accompanied by an increase of T_v and an increase of the residual resistivity ratio. However, among our samples we could not observe crystals with an ideal 122 stoichiometry, as there remains some Si excess on the Pd site. In all cases the transition at T_v rather is a crossover than a second order phase transition, and none of the samples showed signs of a first order transition. This is consistent with $EuPd_2Si_2$ being located at the high pressure side, very close to the critical end point of a line of first order phase transitions in a general p-T diagram for Eu compounds.[5]

SUMMARY

We showed that the intermediate valent, tetragonal $EuPd_2Si_2$ can be grown from a Eu-rich levitating melt using the Czochralski method with an Ar overpressure of 20 bar. The combined chemical and structural analyses revealed that the material grows in a Pd–Si homogeneity range and that this small change of the order of 1 at. % in the composition along the grown ingot of the material has a large impact on the temperature where the valence transition occurs. In this sample, we observe a shift in T_v of about 15 K. Samples with lower T_v formed at the beginning of the growth, while samples with higher T_v formed later in the process. The growth procedure presented here using the Czochralski method will now enable us to provide doped samples and chemically tune this material to further explore the phase diagram, and it shows that $EuPd_2Si_2$ is an excellent candidate for the study of possible critical elasticity.

AUTHOR INFORMATION

Corresponding Author

Kristin Kliemt – *Kristall- und Materiallabor, Physikalisches Institut, Goethe-Universität Frankfurt, 60438 Frankfurt am Main, Germany;* orcid.org/0000-0001-7415-4158; Email: kliemt@physik.uni-frankfurt.de

Authors

Marius Peters – *Kristall- und Materiallabor, Physikalisches Institut, Goethe-Universität Frankfurt, 60438 Frankfurt am Main, Germany*

Isabel Reiser – *Kristall- und Materiallabor, Physikalisches Institut, Goethe-Universität Frankfurt, 60438 Frankfurt am Main, Germany*

Michelle Ocker – *Kristall- und Materiallabor, Physikalisches Institut, Goethe-Universität Frankfurt, 60438 Frankfurt am Main, Germany*

Franziska Walther − *Kristall- und Materiallabor, Physikalisches Institut, Goethe-Universität Frankfurt, 60438 Frankfurt am Main, Germany*
Doan-My Tran − *Kristall- und Materiallabor, Physikalisches Institut, Goethe-Universität Frankfurt, 60438 Frankfurt am Main, Germany*
Eunhyung Cho − *Kristall- und Materiallabor, Physikalisches Institut, Goethe-Universität Frankfurt, 60438 Frankfurt am Main, Germany*
Michael Merz − *Institute for Quantum Materials and Technologies, Karlsruhe Institute of Technology (KIT), 76021 Karlsruhe, Germany; Karlsruhe Nano Micro Facility (KNMFi), Karlsruhe Institute of Technology (KIT), 76344 Eggenstein-Leopoldshafen, Germany;* orcid.org/0000-0002-7346-7176
Amir Abbas Haghighirad − *Institute for Quantum Materials and Technologies, Karlsruhe Institute of Technology (KIT), 76021 Karlsruhe, Germany;* orcid.org/0000-0003-4723-4966
Dominik C. Hezel − *Institut für Geowissenschaften, Petrologie und Geochemie, Goethe-Universität Frankfurt, 60438 Frankfurt am Main, Germany*
Franz Ritter − *Kristall- und Materiallabor, Physikalisches Institut, Goethe-Universität Frankfurt, 60438 Frankfurt am Main, Germany*
Cornelius Krellner − *Kristall- und Materiallabor, Physikalisches Institut, Goethe-Universität Frankfurt, 60438 Frankfurt am Main, Germany*

Notes

The authors declare no competing financial interest.

ACKNOWLEDGMENTS

We thank K.-D. Luther for technical support and R. Möller for proofreading the manuscript. We acknowledge funding by the Deutsche Forschungsgemeinschaft (DFG, German Research Foundation) via the TRR 288 (422213477, projects A03 and B03).

REFERENCES

(1) Kreyssig, A.; et al. Pressure-induced volume-collapsed tetragonal phase of $CaFe_2As_2$ as seen via neutron scattering. *Phys. Rev. B* **2008**, *78*, 184517.
(2) Gati, E.; Garst, M.; Manna, R. S.; Tutsch, U.; Wolf, B.; Bartosch, L.; Schubert, H.; Sasaki, T.; Schlueter, J. A.; Lang, M. Breakdown of Hooke's law of elasticity at the Mott critical endpoint in an organic conductor. *Science Advances* **2016**, *2*, e1601646.
(3) Mimura, K.; Taguchi, Y.; Fukuda, S.; Mitsuda, A.; Sakurai, J.; Ichikawa, K.; Aita, O. Bulk-sensitive high-resolution photoemission study of a temperature-induced valence transition system $EuPd_2Si_2$. *J. Electron Spectrosc. Relat. Phenom.* **2004**, *137−140*, 529.
(4) Adams, D. M.; Heath, A. E.; Jhans, H.; Norman, A.; Leonard, S. The effect of high pressure upon the valence transition in $EuPd_2Si_2$. *J. Phys.: Condens. Matter* **1991**, *3*, 5465.
(5) Ōnuki, Y.; et al. Divalent, trivalent, and heavy fermion states in Eu compounds. *Philos. Mag.* **2017**, *97*, 3399.
(6) Batlogg, B.; Jayaraman, A.; Murgai, V.; Gupta, L.; Parks, R. D.; Croft, M. *Valence instabilities, Pressure-temperature studies and the p-T phase diagram of $EuPd_2Si_2$*, Wachter, P.; Boppart, H., Eds.; North-Holland Publishing Company, 1982; p 229.
(7) Schmiester, G.; Perschied, B.; Kaindl, G.; Zukrowski, J. *Valence Instabilities: Effects of pressure and temperature on the mean valence of $EuPd_2Si_2$*, Wachter, P.; Boppart, H., Eds.; North-Holland Publishing Company, 1982; p 219.
(8) Sampathkumaran, E.; Gupta, L.; Vijayaraghavan, R.; Gopalakrishnan, K.; Pillay, R.; Devare, H. A new and unique Eu-based mixed valence system: $EuPd_2Si_2$. *J. Phys. C: Solid State Phys.* **1981**, *14*, L237.
(9) Mårtensson, N.; Reihl, B.; Schneider, W. D.; Murgai, V.; Gupta, L. C.; Parks, R. D. Highly resolved surface shifts in a mixed-valent system: $EuPd_2Si_2$. *Phys. Rev. B* **1982**, *25*, 1446.
(10) Jhans, H.; Croft, M.; Kemly, E.; Grier, B.; Segre, C. *Theoretical and Experimental Aspects of Valence Fluctuations and Heavy Fermions*; Plenum Press: New York, 1987; p 655.
(11) Vijayakumar, V.; Vaidya, S.; Sampathkumaran, E.; Gupta, L.; Vijayaraghavan, R. Effect of pressure on the electrical resistivity and the thermoelectric power of $EuPd_2Si_2$. *Phys. Lett.* **1981**, *83A*, 469.
(12) Croft, M.; Segre, C.; Hodges, J.; Krishnan, A.; Murgai, V.; Gupta, L.; Parks, R. *Valence instabilities, The phase diagram for a Eu compound undergoing configurational crossover: Mössbauer effect measurements*, Wachter, P.; Boppart, H., Eds.; North-Holland Publishing Company, 1982; p 121.
(13) Segre, C. U.; Croft, M.; Hodges, J. A.; Murgai, V.; Gupta, L. C.; Parks, B. D. Valence Instability in $Eu(Pd_{1-x}Au_x)_2Si_2$: The Global Phase Diagram. *Phys. Rev. Lett.* **1982**, *49*, 1947.
(14) Holland-Moritz, E.; Braun, E.; Roden, B.; Perscheid, B.; Sampathkumaran, E. V.; Langel, W. Neutron scattering, magnetization, and Mössbauer measurements on $EuPd_2Si_2$ with enriched ^{153}Eu isotopes. *Phys. Rev. B* **1987**, *35*, 3122.
(15) Wada, H.; Gomi, H.; Mitsuda, A.; Shiga, M. Specific heat anomaly due to valence transition in $Eu(Pd_{1-x}Pt\ x)_2Si_2$. *Solid State Commun.* **2001**, *117*, 703.
(16) Mazilu, I.; Teresiak, A.; Werner, J.; Behr, G.; Cao, C.; Löser, W.; Eckert, J.; Schultz, L. Phase diagram studies on Er_2PdSi_3 and $ErPd_2Si_2$ intermetallic compounds. *J. Alloys Compd.* **2008**, *454*, 221.
(17) Kuzhel, B.; Belan, B.; Kuzhel, V.; Stets, I.; Serkiz, R. Contribution of unstable valence states of europium to the electronic transport properties of $EuPd_{2-x}Si_{2+x}$. *Chem. Met. Alloys* **2010**, *3*, 83.
(18) Zacharias, M.; Paul, I.; Garst, M. Quantum Critical Elasticity. *Phys. Rev. Lett.* **2015**, *115*, 025703.
(19) Sheldrick, G. M. A Short History of SHELX. *Acta Crystallogr., Sect. A* **2008**, *64*, 112.
(20) Petricek, V.; Dusek, M.; Palatinus, L. Crystallographic Computing System JANA2006: General features. *Z. Kristallogr., Cryst. Mater.* **2014**, *229*, 345.
(21) Kemly, E.; Croft, M.; Murgai, V.; Gupta, L. C.; Godart, C.; Parks, R. D.; Segre, C. U. Mössbauer effects and LIII absorption measurements on $EuPd_2Si_2$. *J. Magn. Magn. Mater.* **1985**, *47*, 403.
(22) Mallik, R.; Sampathkumaran, E.; Strecker, M.; Wortmann, G.; Paulose, P.; Ueda, Y. Complex magnetism in a new alloy, Eu_2PdSi_3, with two crystallographically inequivalent sites. *J. Magn. Magn. Mater.* **1998**, *185*, L135.